STRUCTURAL SCIENCE
CRYSTAL ENGINEERING
MATERIALS

Volume 73 (2017)

Supporting information for article:

Local structure and stacking disorder of chloro-(phthalocyaninato)aluminium

Christian Czech, Lena Kalinowsky and Martin U. Schmidt

S1. Tailor-made force field parameters

The standard Dreiding force field does not have parameters for an Al^{3+} ion with square-planar coordination. Hence, new force field types were added to provide a realistic description of the molecular structure of AlPcCl (see Table S1). The values for all new parameters are shown in 0.

Table S1 Added force field types used for AlPcCl.

force field types	description
C_R1	aromatic C atom of the phthalocyanine moiety (type 1)
C_R2	aromatic C atom of the phthalocyanine moiety (type 2)
C_R3	aromatic C atom of the phthalocyanine moiety (type 3)
N_R1	inner N atom of the phthalocyanine ring (type 1)
N_R2	inner N atom of the phthalocyanine ring (type 2)
N_R3	outer N atom of the phthalocyanine ring

Table S2 Values for all introduced force field types (bond lengths, bond angles and torsion angles) used for AlPcCl.

bond length	R_0 / Å	k_B / (kcal·mol^{-1}·Å^2)
Al3–Cl	2.179	700
Al3–N_R1	1.976	700
Al3–N_R2	1.976	700
C_R1–C_R2	1.407	700
C_R1–N_R3	1.263	700
C_R2–C_R2	1.430	700
C_R2–C_R3	1.463	700
C_R2–H_	1.080	700
C_R3–C_R3	1.409	700
C_R3–H_	1.140	700

N_R1–C_R1	1.442	700
N_R2–C_R1	1.442	700

bond angle	ϑ_0 / °	k_θ / (kcal·mol^{-1})
Al3–N_R1–C_R1	127.827	200
Al3–N_R2–C_R1	127.827	200
C_R1–C_R2–C_R2	108.767	200
C_R1–C_R2–C_R3	123.041	200
C_R1–N_R3–C_R1	127.372	200
C_R1–N_R3–C_R2	125.577	200
C_R2–C_R2–C_R2	115.403	200
C_R2–C_R2–C_R3	123.759	200
C_R2–C_R2–H_	122.496	200
C_R2–C_R3–C_R3	117.102	200
C_R2–C_R3–H_	122.496	100
C_R3–C_R3–C_R3	122.168	200
Cl–Al3–N_R1	102.308	200
Cl–Al3–N_R2	102.308	200
N_R1–Al3–N_R1	156.065	200
N_R1–Al3–N_R2	87.567	200
N_R1–C_R1–C_R2	107.937	200
N_R1–C_R1–N_R3	118.801	200
N_R2–Al3–N_R2	156.065	200
N_R2–C_R1–C_R2	107.937	200
N_R2–C_R1–N_R3	118.801	200
N_R3–C_R1–C_R2	126.528	200

X–C_R3–H_	120.800	100
X–N_R1–X	120.000	100
X–N_R2–X	120.000	100
X–N_R3–X	120.000	100

torsion angle	*B*	*n*	*d*
Cl–Al3–X–X	25	2	−1
X–Al3–N_R1–X	25	2	1
X–Al3–N_R2–X	25	2	1
X–C_R1–C_R2–X	25	2	1
X–C_R1–N_R1–X	25	2	1
X–C_R1–N_R2–X	25	2	1
X–C_R1–N_R3–X	25	2	1
X–C_R2–C_R3–X	25	2	1
X–C_R2–C_R2–X	25	2	1
X–C_R3–C_R3–X	25	2	1

S2. Validation of the force field

The modified force field was tested on the ordered crystal structures ZnPcCl (Mossoyan-Deneux *et al.*, 1985), InPcI (Janczak & Kubiak *et al.*, 1999), TiPcO (Oka *et al.*, 1992) and GaPcCl (Wynne, 1984). A Superposition of these crystal structures and the force field optimised structures are shown in Figure S1 and Figure S2.

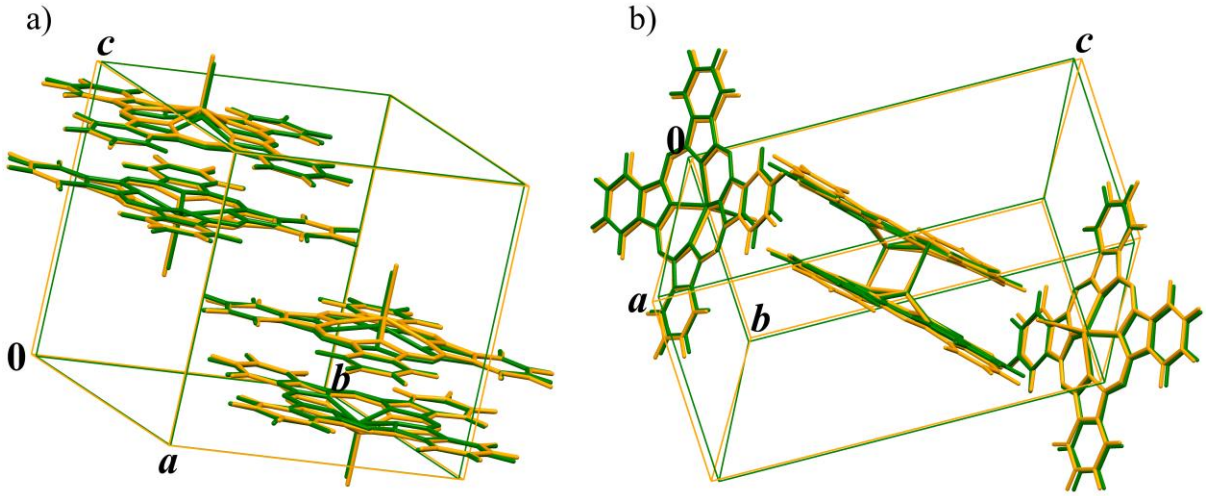

Figure S1 Superposition of crystal structures determined by single-crystal X-ray analysis and force field optimised crystal structures. a) Experimental crystal structure of ZnPcCl (Mossoyan-Deneux *et al.*, 1985) (green), crystal structure optimised by force field (yellow). b) Experimental crystal structure of InPcI (Janczak & Kubiak *et al.*, 1999) (green), crystal structure optimised by force field (yellow).

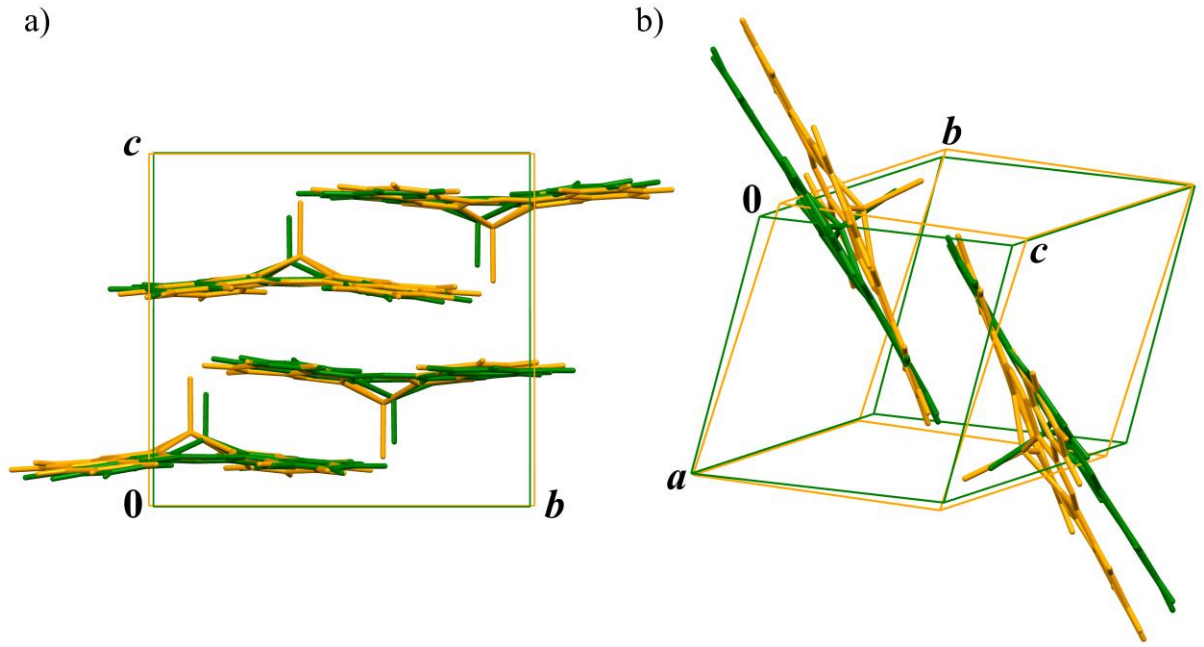

Figure S2 Superposition of crystal structures determined by single-crystal X-ray analysis and force field optimised crystal structures. a) Experimental crystal structure of TiPcO (Oka *et al.*, 1992) (green), crystal structure optimised by force field (yellow). b) Experimental crystal structure of GaPcCl (Wynne, 1984) (green), crystal structure optimised by force field (yellow).

For comparison of the experimental and the energy-minimised crystal structures the root mean square Cartesian displacement (excluding H atoms) is used (van de Streek & Neumann, 2010; van de Streek & Neumann, 2014). The upper r.m.s.c.d. limit for a correct structure must be increased from 0.25 Å

Table S3 R.m.s. Cartesian displacements of the force field minimised structures *versus* the experimental crystal structures.

CSD-refcode	Compound	r.m.s.c.d. value / Å	
		fixed unit cell	free unit cell
DAMTEQ	ZnPcCl	0.1865	0.2174
BIJQOA	InPcI	0.1366	0.1404
BITSAY02	TiPcO	0.4791	0.4576
CUWNUD	GaPcCl	0.1352	0.4089

The experimental crystal structures of ZnPcCl and InPcI were reproduced very well and the r.m.s.c.d. values are small. After optimisation of the crystal structure of TiPcO, the packing in principle is reproduced well, but the molecules are slightly shifted resulting in an increased r.m.s.c.d. value. In the structure of GaPcCl the molecules of the structure optimised by the force field are inclined to their original position. Therefore the r.m.s.c.d. value is large. But in principal the arrangement of the molecules agree with the experimental one.

S3. Calculation of stacking probabilities

For the stacking sequences, an additive combination of energies is assumed, i.e. the energy of a given double-layer depends almost exclusively only on the arrangement of the neighbouring layers, whereas interactions with more distant double-layers do not play a major role. For a given length of the local stacking motif, we use a combinatorial approach to get the total number of possible local stacking motifs (Teteruk *et al*, 2014).

For a statistical examination of the energies of the stacking motifs, the Boltzmann distribution is used.

$$\frac{N_i}{N_j} = \frac{g_i}{g_j} \mathrm{e}^{\frac{E_i - E_j}{kT}}$$

Using the energies of the stacking motifs, first the relative occupancy values N_i and afterwards stacking probabilities p_i for each local stacking motif was calculated.

$$p_i = \frac{N_i}{\sum_{i=1}^{n} N_i}$$

As the basis we took the DFT-D optimised models '1111' with Z = 2, '1212' with Z = 4 and '1221' with Z = 8. On a given double-layer the obtained stacking probabilities describe the chance to find a specific neighbouring double-layer within a theoretical infinite disordered crystal. The resulting stacking probabilities are given in Table S4.

Table S4 Probabilities for local stacking motifs. The Energies are given in kJ·mol^{-1} per double-layer.

Local stacking motif	E_{rel} of the local stacking motif kJ·mol^{-1}	Probability of the local stacking motif
111	3.40	0.06
112	2.13	0.10
121	0.00	0.24
122	2.13	0.10
211	2.13	0.10
212	0.00	0.24
221	2.13	0.10
222	3.40	0.06

S4. Calculation of the interaction between the 1st and 3rd double-layers

The interaction energy between the 1st and the 3rd double-layers connected by a shift of $\boldsymbol{t}_1 + \boldsymbol{t}_2$ were calculated using the model '12'. The ***c*** axis was quadrupled (***c***' = 4***c***), so that the unit cell include 8 double-layers. All molecules, except those in 1st and 3rd double-layers, were removed. The energy was calculated with force field methods without optimising the cell parameters and coordinates of all atoms. Afterwards the 3rd double-layer were shifted in such a way, that it corresponds to a shift of $2 \cdot \boldsymbol{t}_1$ (related to the 1st double-layer). The energy was calculated in the same way as before. This is the interaction energy between the 1st and the 3rd double-layers connected by a shift of $2 \cdot \boldsymbol{t}_1$.

References

Janczak, J., Kubiak, R. (1999). *Inorg.Chim.Acta* **288**, 174–180.

Mayo, S. L., Olafson, B. D., Goddard III, W. A. (1990). *J. Phys. Chem.* **94**, 8897-8909.

Mossoyan-Deneux, M., Benlian, D., Pierrot, M., Fournel, A., Sorbier, J. P. (1985). *Inorg. Chem.* **24**, 1878–1882.

Oka, K., Okada, O. Nukada, K. (1992). *Jpn. J. Appl. Phys.* **31**, 2181–2184.

Teteruk, J. L., Glinnemann, J., Heyse, W., Johansson, K. E., van de Streek, J., Schmidt, M. U. (2014). *Acta Cryst.* B**70**, 296–305.

Wynne, K. J. (1984). *Inorg.Chem.* **23**, 4658–4663.

Van de Streek, J., Neumann, M. A., (2010). Acta Cryst. B**66**, 544–558.

Van de Streek, J., Neumann, M. A., (2014). Acta Cryst. B**70**, 1020–1032.